replacement phases were improved and extended from 5 to 3.5 Å by sevenfold averaging and solvent flattening with the program DM (*24*). Phases were extended in a total of 150 cycles. The resulting maps were readily interpretable, and most of the polypeptide could be easily fitted into the density with the program 'O' (*25*). The model was refined by using X-PLOR (*26*) with noncrystallographic constraints and restraints. The model contains 92 out of 99 residues in three different fragments. Refinement with one "group temperature factor" per residue, and an overall anisotropic temperature factor, decreased the *R* factor (for 7870 reflections) to 0.23 and the R_{free} (for 903 randomly chosen reflections) to 0.38 (*26*). The root-mean-square (rms) deviations from ideality for bond lengths and angles are 0.018 Å and 2.8°, respectively. The rms deviation between Cα atoms of different subunits in the heptamer is 0.51 Å and between all atoms 0.66 Å. The only outlying residues in the Ramachandran map belong to the flexible loop comprising residues 17 to 33, which is partially disordered in the structure, and Glu^9, which is located in a tight turn. A three-dimensional–one-dimensional profile (*27*) shows a better-than-average score for a protein of this size, with no negative values (*28*). The only region with a somewhat low score is the flexible loop. A specific-sequence marker is provided by the single mercury position per subunit in the heavy atom derivative, which is close to the side chain nitrogen of Trp^{50} (there are neither histidines nor cysteines in MI-cpn10). Crystals of selenomethionine–MI-cpn10 were obtained but did not result in significant peaks in difference Pattersons and difference Fouriers after data collection with multiwavelength anomalous diffraction techniques. Apparently the mobility and disorder of the single Met^{22} in the flexible loop was still too large. In our structure, we see some density that must be part of this flexible loop, but the precise way in which it is connected to the remainder of the molecule is still uncertain. Figures are drawn with MOLSCRIPT and RASTER3D (*29*).

13. S. Landry *et al.*, *Nature* **364**, 255 (1993).
14. O. Kovalenko, O. Yifrach, A. Horovitz, *Biochemistry* **33**, 14974 (1994).
15. J. Kim and R. L. Modlin, in preparation.
16. S. Chen *et al.*, *Nature* **371**, 261 (1994); J. R. Harris, R. Zahn, A. Plückthun, *J. Struct. Biol.* **115**, 68 (1995); T. Langer *et al.*, *EMBO J.* **11**, 4757 (1992).
17. S. M. van der Vies *et al.*, *Nature* **368**, 654 (1994).
18. G. Fossati *et al.*, *J. Biol. Chem.* **270**, 26159 (1995).
19. W. A. Fenton *et al.*, *Nature* **371**, 614 (1994).
20. E. S. Bochkareva and A. S. Girshovich, *J. Biol. Chem.* **267**, 25672 (1992).
21. J. S. Weissman *et al.*, *Cell* **83**, 577 (1995).
22. Evidence for hydrophobic interactions between GroEL and substrate protein has been reported by several groups including M. K. Hayer-Hartl *et al.*, *EMBO J.* **13**, 3192 (1994); Z. Lin *et al.*, *J. Biol. Chem.* **270**, 1011 (1995).
23. "The CCP4 suite: Programs for protein crystallography," *Acta Crystallogr.* **D50**, 760 (1994).
24. K. Cowtan, Joint CCP4 and ESF-EACBM, *Newsl. Prot. Crystallogr.* **31**, 34 (1994).
25. T. A. Jones *et al.*, *Acta Crystallogr.* **A47**, 110 (1991).
26. A. Brünger, X-PLOR User Manual (Yale Univ. Press, New Haven, CT, 1990); *Nature* **355**, 472 (1992).
27. R. Lüthy *et al.*, *Nature* **356**, 83 (1992).
28. S. C. Mande, V. Mehra, B. R. Bloom, W. G. J. Hol, data not shown.
29. MOLSCRIPT: P. J. Kraulis, *J. Appl. Crystallogr.* **24**, 946 (1991); RASTER3D: D. J. Bacon and W. F. Anderson, *J. Mol. Graphics* **6**, 219 (1988); E. A. Merritt *et al.*, *Acta Crystallogr.* **D50**, 869 (1994).
30. Abbreviations for the amino acid residues are as follows: A, Ala; C, Cys; D, Asp; E, Glu; F, Phe; G, Gly; H, His; I, Ile; K, Lys; L, Leu; M, Met; N, Asn; P, Pro; Q, Gln; R, Arg; S, Ser; T, Thr; V, Val; W, Trp; and Y, Tyr.
31. Genetic Computer Group, Incorporated, copyright 1982–1992, Madison, WI, USA.
32. A. L. Hughes, *Mol. Biol. Evol.* **10**, 1343 (1993).
33. We thank the members of the Biomolecular Structure Center for support regarding synchrotron and computing aspects of these studies, in particular S. Turley, C. Verlinde, and E. Merritt. The assistance of I. Feil in site-directed mutagenesis studies is appreciated. Access to the Stanford Synchrotron Radiation Laboratories is gratefully acknowledged. This work was supported by NIH grants AI07118 and 23545, the Howard Hughes Medical Institute, the Immunology of Mycobacteria (IMMMYC) program of the United Nations Development Programme–World Bank–World Health Organization Special Program for Research and Training in Tropical Diseases, a major equipment grant from the Murdock Charitable Trust to the Biomolecular Structure Center, and by the School of Medicine of the University of Washington, Seattle, WA. The coordinates for *M. Leprae* cpn10 have been deposited with the Brookhaven Protein Data Bank.

27 November 1995; accepted 15 December 1995

Protection Against Osmotic Stress by cGMP-Mediated Myosin Phosphorylation

Hidekazu Kuwayama, Maria Ecke, Günther Gerisch, Peter J. M. Van Haastert*

Conventional myosin functions universally as a generator of motive force in eukaryotic cells. Analysis of mutants of the microorganism *Dictyostelium discoideum* revealed that myosin also provides resistance against high external osmolarities. An osmo-induced increase of intracellular guanosine 3′,5′-monophosphate was shown to mediate phosphorylation of three threonine residues on the myosin tail, which caused a relocalization of myosin required to resist osmotic stress. This redistribution of myosin allowed cells to adopt a spherical shape and may provide physical strength to withstand extensive cell shrinkage in high osmolarities.

Cells exposed to osmotic stress can avoid dehydrative collapse either by using a cell wall (*1*) or by increasing the intracellular osmotic potential by synthesis of small molecules like glycerol, uptake of ions, or discharge of water (*2*). Actin and some of its binding proteins are required to resist high osmotic stress in yeast (*3*). The other major component of the cytoskeleton, myosin II or conventional myosin, exerts motive force by interacting with actin filaments (*4*). *Dictyostelium discoideum* is a microorganism with a small haploid genome from which mutants altered in cytoskeletal proteins have been isolated (*5–7*). Studies of mutants lacking myosin II heavy chain (mhc^-) reveal that this form of myosin is essential for cytokinesis, capping of cell surface lectin receptors, and normal cell motility and chemotaxis (*5*, *8*, *9*). Here we have used *D. discoideum* to investigate the role of myosin II in protecting amoeboid cells from high osmotic pressure.

Wild-type XP55 cells resisted an osmotic shock of 300 mM glucose for ~30 min; 50% of the cells died after a shock of about 60 min (Fig. 1A). In contrast, mhc^- cells were very sensitive to osmotic stress with a 50% reduction of cell viability after 5 to 10 min (Fig. 1A). Cells of the mhc^- mutant that had been transfected with complementary DNA (cDNA) encoding normal myosin II heavy chains (mhc^{wt}) showed a viability comparable to that of the wild-type XP55 (Fig. 1A).

Myosin II filaments bind to actin filaments more effectively than myosin monomers (*10*, *11*). Phosphorylation of myosin II at three threonine residues of its tail region inhibits filament formation (*10*, *12*) and thus weakens the interaction with actin filaments. Mutant mhc^{AAA} produces a myosin II heavy chain in which the phosphorylatable threonines are replaced by alanine residues. As a consequence of this mutation, myosin II exists predominantly in the filamentous state, and the assembly and disassembly rate are probably strongly reduced (*9*, *10*). These mhc^{AAA} cells showed the same sensitivity to high concentrations of glucose as mhc^- cells (Fig. 1A), which suggests that phosphorylation of myosin II at its tail was required to protect cells against osmotic stress (*13*).

Guanosine 3′,5′-monophosphate (cGMP) acts as a universal second messenger in eukaryotic cells (*14*). In *D. discoideum*, cGMP levels increase upon stimulation with the chemoattractant adenosine 3′,5′-monophosphate (cAMP) (*15*). Intracellular cGMP regulates the assembly and disassembly of myosin filaments by inducing the phosphorylation of the threonine residues (*16*). Osmotic stress also activates guanylyl cyclase in wild-type *D. discoideum* cells; the cGMP concentration increased after 1 min and reached a peak at ~10 min after the onset of stimulation (*17*) (Fig. 1B). A transient accumulation of cGMP levels upon addition of 300 mM glucose was also observed in wild-type XP55 and in the mhc^{wt}, mhc^-, and mhc^{AAA} strains (Fig. 1B). No increase of cGMP levels was found in the nonchemotactic mutant KI-8 in which gua-

H. Kuwayama and P. J. M. Van Haastert, Department of Biochemistry, University of Groningen, Nijenborgh 4, 9747 AG Groningen, Netherlands.
M. Ecke and G. Gerisch, Max-Planck-Institut für Biochemie, D-82143 Martinsried, Germany.

*To whom correspondence should be addressed.

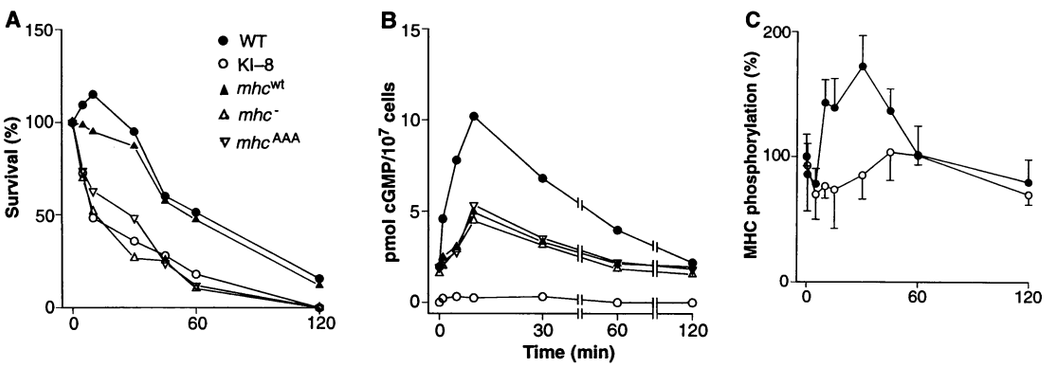

Fig. 1. Time course of (**A**) survival, (**B**) cGMP accumulation, and (**C**) myosin II heavy chain (MHC) phosphorylation in the presence of 300 mM glucose for wild-type XP55 and mutants KI-8, *mhc*^{wt}, *mhc*$^{-}$, and *mhc*^{AAA} of *D. discoideum* (*30*). Survival and myosin II phosphorylation are presented as percent of unstimulated cells. Results in (C) are the means ± SD of three independent experiments with triplicate determinations.

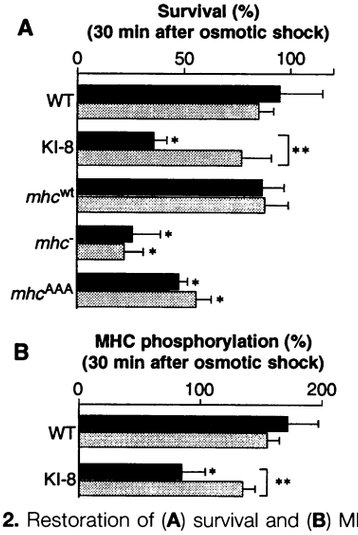

Fig. 2. Restoration of (**A**) survival and (**B**) MHC phosphorylation by the cell-permeable cGMP analog 8Br-cGMP (*31*). Survival and myosin II phosphorylation are presented as percent of unstimulated cells. Solid bar, control; stippled bar, 8Br-cGMP. Statistical analysis: Asterisk indicates $P < 0.01$, which is significantly lower than in wild-type (WT) cells; double asterisk indicates $P < 0.05$, which is significantly higher than without 8Br-cGMP. Results are the means ± SD of three independent experiments with triplicate determinations.

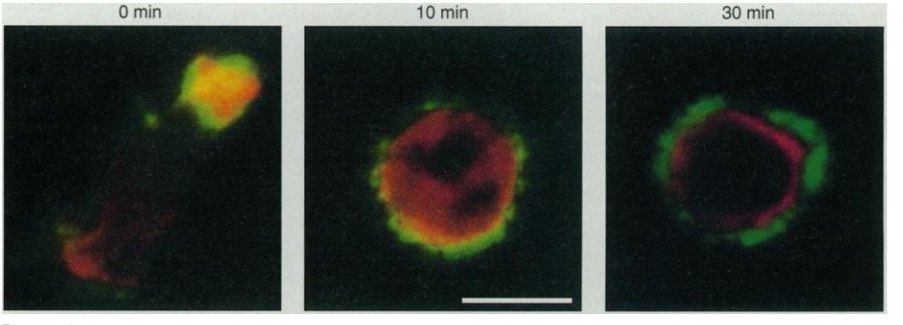

Fig. 3. Cell shape and localization of myosin II (red) and actin filaments (green) in XP55 cells before and after an osmotic shock with 300 mM glucose (*32*). A confocal section was made through the center of the cell; areas where myosin II and actin filaments colocalized are yellow. Bar, 5 μm.

nylyl cyclase activity is strongly reduced (*18*). To investigate the role of cGMP in osmoregulation, we tested the survival of this mutant under conditions of osmotic stress. Mutant KI-8 cells proved to be very sensitive to osmotic stress; survival of these cells was reduced by an amount similar to that seen in *mhc*$^{-}$ mutants (Fig. 1A). Moreover, 300 mM glucose induced the transient phosphorylation of myosin II in wild-type XP55 cells, which was already detectable after 2 min, whereas mutant KI-8 showed no response (Fig. 1C). A cell-permeable cGMP analog, 8-bromoguanosine 3′,5′-monophosphate (8Br-cGMP), was added to these mutants in combination with 300 mM glucose. Whereas the survival of XP55, *mhc*^{wt}, *mhc*$^{-}$, and *mhc*^{AAA} was not influenced by 1 mM 8Br-cGMP, the analog restored the survival of mutant KI-8 (Fig. 2A). Half-maximal restoration was induced by ~100 mM 8Br-cGMP and was specific for this cell-permeable cGMP analog (*19*). In addition, 8Br-cGMP in the presence of glucose induced myosin II phosphorylation in KI-8 cells (Fig. 2B). Thus, a cell-permeable cGMP analog restored osmosensitivity in the guanylyl cyclase mutant but not in the myosin mutants.

The distribution of the cytoskeletal proteins actin and myosin was analyzed by confocal fluorescence microscopy with labeled phalloidin to stain actin filaments and monoclonal antibodies to label myosin II (Fig. 3). Control cells were highly motile and elongated with many pseudopodial extensions. Actin filaments were localized primarily in the extending pseudopodia (*20*), whereas myosin II was found throughout the cytoplasm and enriched in pseudopodia. At 10 min after the osmotic shock with 300 mM glucose, cells shrank by ~50% (*21*), assuming a rigid state in which a more spherical core region was surrounded by flattened extensions. Filamental actin remained in the extensions. Myosin II moved within 10 min toward the cortex of the core; dual labeling revealed that myosin II was localized primarily in a layer beneath the actin-rich cortex.

Thus, we propose the following model: Osmotic stress induces the activation of guanylyl cyclase. The main function of the produced cGMP is to mediate myosin II phosphorylation at three threonine residues on its tail, which enhances the disassembly of myosin II filaments and thereby recruits myosin for deposition below a peripheral layer of actin filaments. *Dictyostelium discoideum* cells respond chemotactically to cAMP. Guanylyl cyclase and myosin II phosphorylation are essential for both osmo- and chemosensory transduction. Activation of guanylyl cyclase by these signals must use different mechanisms because chemotactic signal transduction is ablated in mutants lacking the heterotrimeric guanosine triphosphate binding protein (G protein) subunits Gα2 (*22*) or Gβ (*23*), which show a normal response to osmotic stress (*24*). In yeast, osmosensing is mediated by a two-component system composed of a histidine kinase and its receiver domain (*25*). In the yeast system, the sensor mediates osmoregulation through the production of glycerol. Recently, a gene encoding a putative histidine kinase has been identified in *D. discoideum*; interestingly, a mutant with a disruption of this gene is sensitive to high osmolarities (*26*). Possibly, this two-component system is a common constituent of the osmosensory pathways, including the one that controls the actin and myosin system shown here.

REFERENCES AND NOTES

1. H. E. Street and H. Öpik, *The Physiology of Flowering Plants* (Arnold, London, ed. 3, 1984).
2. W. H. Mager and J. C. S. Varela, *Mol. Microbiol.* **10**, 253 (1993); M. C. Gustin, X.-L. Zhou, B. Martinac, C.

Kung, *Science* **242**, 762 (1988); M. J. Chrispeels and P. Agre, *Trends Biochem. Sci.* **19**, 421 (1994).
3. P. Novick and D. Botstein, *Cell* **40**, 415 (1985); S. Chowdhury, K. W. Smith, M. C. Gustin, *J. Cell Biol.* **118**, 561 (1992).
4. J. A. Spudich, *Cell Regul.* **1**, 1 (1989).
5. A. De Lozanne and J. A. Spudich, *Science* **236**, 1086 (1987); D. J. Manstein, M. A. Titus, A. De Lozanne, J. A. Spudich, *EMBO J.* **8**, 923 (1989).
6. W. Witke, M. Schleicher, A. A. Noegel, *Cell* **68**, 53 (1992); D. Cox *et al.*, *J. Cell Biol.* **116**, 943 (1992).
7. E. L. De Hostos *et al.*, *J. Cell Biol.* **120**, 163 (1993).
8. C. Pasternak, J. A. Spudich, E. L. Elson, *Nature* **341**, 549 (1989).
9. G. Gerisch *et al.*, *Soc. Exp. Biol.* 297 (1993).
10. T. Truong, Q. G. Medley, G. P. Côté, *J. Biol. Chem.* **267**, 9767 (1992).
11. D. Lück-Vielmetter, M. Schleicher, B. Grabatin, J. Wippler, G. Gerisch, *FEBS Lett.* **269**, 239 (1990).
12. C. Pasternak, P. F. Flicker, S, Ravid, J. A. Spudich, *J. Cell Biol.* **109**, 203 (1989); T. T. Egelhoff, R. J. Lee, J. A. Spudich, *Cell* **75**, 363 (1993).
13. *mhc*$^-$ cells grown in axenic conditions are larger than wild-type cells. However, this increased size was not the reason for their sensitivity to osmotic damage, because *mhc*$^-$ cells grown on bacteria or the *mhc*^{AAA} mutant cells were similar in size to wild-type AX2 cells (*21*), but both were still osmosensitive.
14. P. M. W. Janssens and P. J. M. Van Haastert, *Microbiol. Rev* **51**, 396 (1987).
15. J. M. Mato, F. A. Krens, P. J. M. Van Haastert, T. M. Konijn, *Proc. Natl. Acad. Sci. U.S.A.* **74**, 2348 (1977).
16. G. Liu, H. Kuwayama, S. Ishida, P. C. Newell, *J. Cell Sci.* **106**, 591 (1993).
17. M. Oyama, unpublished observation.
18. H. Kuwayama, S. Ishida, P. J. M. Van Haastert, *J. Cell Biol.* **123**, 1453 (1993).
19. The more polar cGMP and S_p-cGMPS (guanosine 3′,5′-monophosphorothioate, S_p-isomer) and the corresponding cAMP analogs had no significant effect at a concentration of 1 mM.
20. S. Yumura and Y. Fukui, *Nature* **314**, 194 (1985).
21. The volume of AX2 and *mhc*^{AAA} cells was measured with a Haematokrit and was identical within the statistical error of 10%. An osmotic shock of 0.3 M glucose induced a reduction in volume of 46 ± 3% and 52 ± 2% in AX2 and *mhc*^{AAA} cells, respectively.
22. A. Kumagai *et al.*, *Cell* **57**, 265 (1989).
23. L. Wu, R. Valkema, P. J. M. Van Haastert, P. N. Devreotes, *J. Cell Biol.* **129**, 1667 (1995).
24. H. Kuwayama and P. J. M. Van Haastert, unpublished observation.
25. T. Maeda, S. M. Wurgler-Murphy, H. Saito, *Nature* **369**, 242 (1994); T. Maeda, M. Takekawa, H. Saito, *Science* **269**, 554 (1995).
26. S. C. Schuster, A. Noegel, G. Gerisch, M. I. Simon, unpublished observation.
27. P. J. M. Van Haastert and P. R. Van Der Heijden, *J. Cell Biol.* **96**, 347 (1983).
28. A. Jungbluth *et al.*, *J. Cell Sci.* **107**, 117 (1994).
29. K. Pagh and G. Gerisch, *J. Cell Biol.* **103**, 1527 (1986).
30. The following cell lines were used: Mutant KI-8 has reduced guanylyl cyclase activity and is derived from wild-type strain XP55 (*18*); the myosin II null mutant *mhc*$^-$ (strain HS2205); transformant *mhc*^{wt} in which wild-type myosin II is expressed in *mhc*$^-$ cells (strain HG1554); and transformant *mhc*^{AAA} expressing in *mhc*$^-$ cells a mutant myosin II with the three threonine phosphorylation sites mutated to alanine residues (strain HG1555) (*9*). Cells were cultivated in tissue culture plate in HL5 defined medium (*mhc*$^-$, *mhc*^{wt}, *mhc*^{AAA}, and AX2) (*7*) or on 1/3 SM agar plates [0.3% glucose, 0.3% peptone, 1.5% agar, and 40 mM KH_2PO_4-Na_2HPO_4 (pH 6. 0)] with *Escherichia coli* B/r (KI-8 and XP55). The cells were removed from the plates with phosphate buffer [10 mM K_2HPO_4-NaH_2PO_4 (pH 6. 5) (Fig. 1, A and B)] or MES buffer [20 mM MES, 2 mM $MgSO_4$, 0. 2 mM $CaCl_2$ (pH 6.15) (Fig. 1C)]. Cells were shaken in these buffers at a density of 10^7 cells per milliliter for 1 hour, washed three times, and resuspended in the respective buffers at 10^7 cells per milliliter (Fig. 1A) or 10^8 cells per milliliter (Fig. 1, B and C), and then stimulated with 300 mM glucose. Survival was measured by 1000-fold dilution of cells at the time indicated, followed by plating 200 cells on a 1/3 SM plate with *E. coli* and counting colonies several days later. Intracellular accumulation of cGMP was measured by isotope dilution assay (*27*). Phosphorylation of myosin II heavy chain was determined by labeling cells with ^{32}P, lysis of the cells at the time indicated, followed by immunoprecipitation of myosin with monoclonal antibody JIG-3 to myosin II as described (*15*).
31. In (A), cells were incubated with 300 mM glucose for 30 min in the absence or presence of 1 mM 8Br-cGMP. The survival of XP55, KI-8, *mhc*^{wt}, *mhc*$^-$, and *mhc*^{AAA} cells was determined as described in Fig. 1. In (B), phosphorylation of myosin II heavy chain was induced in XP55 and KI-8 cells upon incubation with 300 mM glucose with or without 1 mM 8Br-cGMP.
32. Cells were starved for 1 hour in phosphate buffer, incubated in the presence of 300 mM glucose for 10 min and 30 min, and fixed with 15% picric acid and 2% formaldehyde in 10 mM Pipes-HCl (pH 6.0) (*28*). The fixed cells were incubated simultaneously with fluorescein isothiocyanate–conjugated phalloidin to stain actin filaments and with monoclonal antibody 396 to myosin II [which recognizes both myosin II monomers and filaments (*29*)] plus tetramethyl rhodamine isothiocyanate–conjugated goat antibody to mouse immunoglobulin G. Confocal sections of cells were taken with a 40× Plan-Neofluar objective on a Zeiss LSM 410 fluorescence laser-scanning microscope; the images were color-labeled to red (myosin II) and green (actin).
33. We thank P. C. Newell for monoclonal antibody JIG-3 and M. Oyama for useful comments. The *mhc*^{AAA} transformant was produced by D. Vielmetter in collaboration with J. A. Spudich, and KI-8 was isolated by H.K. in collaboration with S. Ishida. Supported in part by grant SFB266/D7 of the Deutsche Forschungsgemeinschaft.

11 August 1995; accepted 10 November 1995

Regulation of PHO4 Nuclear Localization by the PHO80-PHO85 Cyclin-CDK Complex

Elizabeth M. O'Neill, Arie Kaffman, Emmitt R. Jolly, Erin K. O'Shea*

PHO4, a transcription factor required for induction of the *PHO5* gene in response to phosphate starvation, is phosphorylated by the PHO80-PHO85 cyclin-CDK (cyclin-dependent kinase) complex when yeast are grown in phosphate-rich medium. PHO4 was shown to be concentrated in the nucleus when yeast were starved for phosphate and was predominantly cytoplasmic when yeast were grown in phosphate-rich medium. The sites of phosphorylation on PHO4 were identified, and phosphorylation was shown to be required for full repression of *PHO5* transcription when yeast were grown in high phosphate. Thus, phosphorylation of PHO4 by PHO80-PHO85 turns off *PHO5* transcription by regulating the nuclear localization of PHO4.

The transcription of *PHO5*, which encodes a secreted acid phosphatase, is tightly repressed when *Saccharomyces cerevisiae* are grown in phosphate-rich medium, and its induction is more than 100-fold increased when yeast are starved for phosphate (*1*). Transcriptional induction of *PHO5* requires the transcription factor PHO4, and correlative evidence suggests that PHO4 activity is negatively regulated by phosphorylation (*2*). When yeast are grown in phosphate-rich medium, the PHO80-PHO85 cyclin-CDK (cyclin-dependent kinase) complex phosphorylates PHO4 (*2*) and transcription of *PHO5* is repressed. When yeast are starved for phosphate, the kinase activity of the PHO80-PHO85 complex is down-regulated by the CDK inhibitor PHO81 (*3*). This reduced activity results in the appearance of an underphosphorylated form of PHO4 (*2*) that, in combination with a second transcription factor, PHO2, binds to the *PHO5* promoter and activates *PHO5* transcription (*4*).

We wished to determine how changes in phosphate availability affect PHO4 function. Phosphate starvation does not have a large effect on PHO4 stability; no difference in the amount of PHO4 is observed between yeast grown in low versus high phosphate medium (*2*). Because PHO4 occupies binding sites in the *PHO5* promoter in vivo under inducing, but not repressing, conditions (*5*), the phosphate signal is likely to affect PHO4 function at the level of DNA binding or some prior step, such as nuclear localization. Preliminary data suggest that phosphorylated and unphosphorylated PHO4 have a similar affinity for DNA (*6*).

We therefore examined the subcellular localization of PHO4 in wild-type cells grown in low or high phosphate medium. PHO4 is concentrated in the nucleus when yeast are starved for phosphate and is largely cytoplasmic when yeast are grown in phosphate-rich medium (Fig. 1, A to D). In *pho80*Δ and *pho85*Δ strains, in which PHO4 is not phosphorylated (*2*) and which express *PHO5* constitutively (*1*), PHO4 was concentrated in the nucleus, even when the strains were grown in phosphate-rich medium (*6*). In contrast, PHO4 was predominantly cytoplasmic in a *pho81*Δ strain grown in high or low phosphate conditions (*6*). In this strain, PHO4 is phosphorylated even when yeast are starved for phosphate (*2*),

Department of Biochemistry and Biophysics, University of California at San Francisco, School of Medicine, San Francisco, CA 94143–0448, USA.

*To whom correspondence should be addressed.